

1 **Interpolation algorithm ranking using cross-validation**  
2 **and the role of smoothing effect. A coal zone example**

3 Oriol Falivene<sup>1,3</sup>, Lluís Cabrera<sup>1</sup>, Raimon Tolosana-Delgado<sup>2</sup>, Alberto Sáez<sup>1</sup>

4 <sup>1</sup> Geomodels Institute. Group of Geodynamics and Basin Analysis. Dept. EPGM. Universitat de Barcelona, c/ Martí i  
5 Franquès s/n, Facultat de Geologia, 08028, Barcelona, Spain. email: [oriolfalivene@ub.edu](mailto:oriolfalivene@ub.edu)

6 <sup>2</sup> Laboratory of Marine Engineering, Technical University of Catalunya, 08034 Barcelona (Spain)

7 <sup>3</sup> Presently at Shell International Exploration and Production, Kessler Park 1, 2280 AB, Rijswijk (The Netherlands).  
8 Email address: [oriol.falivene@shell.com](mailto:oriol.falivene@shell.com)

9 **Corresponding Author:** Oriol Falivene

10 **ABSTRACT**

11 For a property measured at several locations, interpolation algorithms provide a  
12 unique and smooth function yielding a locally realistic estimation at any point within  
13 the sampled region. Previous studies searching for optimal interpolation strategies by  
14 measuring cross-validation error have not found consistent rankings; this fact was  
15 traditionally explained by differences in the distribution, spatial variability and sampling  
16 patterns of the datasets. This article demonstrates that ranking differences are also  
17 related to interpolation smoothing, an important factor controlling cross-validation  
18 errors that was not considered previously. Indeed, smoothing in average-based  
19 interpolation algorithms depends on the number of neighbouring data points used to  
20 obtain each interpolated value, among other algorithm parameters. A 3D dataset of  
21 calorific value measurements from a coal zone is used to demonstrate that different  
22 algorithm rankings can be obtained solely by varying the number of neighbouring points  
23 considered (i.e. whilst maintaining the distribution, spatial variability and sampling  
24 pattern of the dataset). These results suggest that cross-validation error cannot be used  
25 as a unique criterion to compare the performance of interpolation algorithms, as has

26 been done in the past, and indicate that smoothing should be also coupled to search for  
27 optimum and geologically realistic interpolation algorithms.

28 **Keywords:** interpolation, cross-validation, smoothing effect, Kriging, inverse distance  
29 weighting

## 30 1. INTRODUCTION

31 Interpolation algorithms aim to predict the value of a property at a location by  
32 using values of the same property sampled at scattered neighbouring points (Journel and  
33 Huijbregts, 1978; Jones et al., 1986; Davis, 2002). These algorithms yield a unique  
34 (though different for each method) property map honouring input data. Interpolation in  
35 geosciences is widely used for both predictive and visualization purposes. A variety of  
36 algorithms have been developed to carry out interpolations (Morrisson, 1974), for  
37 example inverse distance weighting (IDW, Kane et al., 1982), Kriging, (Matheron,  
38 1963), splines (Ahlberg et al., 1967; Mitasova and Mitas, 1993) or polynomial  
39 regression.

40 The selection of optimal interpolation strategies for continuous variables is an  
41 important and ongoing subject of debate (Lu and Wong, 2008; Bater and Coops, 2009).  
42 Cross-validation (CV) has often been used to compare the performance of interpolation  
43 algorithms (Table 1). CV is based on calculating the value of the variable at locations  
44 where the true value is known, but has been temporally removed from the input data,  
45 and then measuring the CV error by comparing the estimated value against the true one  
46 (Davis, 1987; Isaaks and Srivastava, 1989). Past comparisons based on CV error have  
47 yielded a variety of results, not always consistent (Table 1). For instance, in comparison  
48 of two widely used algorithms such as Kriging and IDW, some authors have found that  
49 Kriging yields better interpolations (Weber and Englund, 1994; Zimmerman et al.,

50 1999; Goovaerts, 2000; Teegavarapu and Chandramouli, 2005; Lu and Wong, 2008),  
51 some have not found any significant differences in the results (Dirks et al., 1992;  
52 Moyeed and Papritz, 2002; Gallichand and Marcotte, 1993), and others have found that  
53 IDW yields better interpolations (Weber and Englund, 1992; Lu and Wong, 2008).

#### 54 TENTATIVE POSITION FOR TABLE 1

55 The disparity in the results obtained from existing interpolation algorithm  
56 rankings using CV error (Table 1) motivated this research. We demonstrate that the  
57 comparisons solely based on CV error are utterly flawed. Apart from the fact that  
58 rankings may depend on some specific characteristics of the particular data set used for  
59 the comparison, we provide evidence that the size of the search neighbourhood plays a  
60 determinant role in algorithm rankings considering only CV error. The search  
61 neighbourhood is amongst the factors controlling the smoothing effect of each  
62 interpolation strategy. These findings challenge the practice of ranking and qualifying  
63 interpolation algorithms considering CV error (Table 1), and show that there is no  
64 absolute best interpolation algorithm: one has to establish a trade-off between minimum  
65 CV error and predictions with low smoothing. A representative example, derived from a  
66 real 3D dataset with calorific values from a coal mine, is used for illustration purposes  
67 (Figure 1).

#### 68 TENTATIVE POSITION FOR FIGURE 1

## 69 2. METHODS

70 For our rankings, we considered two commonly used interpolation algorithms:  
71 IDW and Ordinary Kriging. Both methods provide an estimate  $Z^*$  of the studied variable

72  $Z(x_0)$  at an unsampled location  $x_0$ , by means of a linear combination of  $N$  observed  
73 values of  $Z$ , denoted as  $z_1, z_2, \dots, z_N$ ,

$$Z^*(x_0) = \sum w_i \cdot z_i \quad (1)$$

74 For both algorithms compared, several numbers of averaged neighbours,  $N$ ,  
75 ranging from 1 (nearest neighbour) to 288 were considered. Apart from well data  
76 locations (Figure 1B), interpolations were also carried out over the whole three-  
77 dimensional grid (Figure 1D) to attach a visual representation to the interpolation  
78 strategies compared by CV.

79 IDW is a straightforward and simple interpolation method, in which the weights  
80  $w_i$  of Eq. (1) for each averaged neighbouring data point are assigned according to an  
81 inverse of distance criterion (Kane et al., 1982).

$$w_i = \beta^{-1} \cdot d^\alpha(x_i, x_0), \quad \text{where } \beta = \sum d^\alpha(x_i, x_0)$$

82 Several distance weighting power factors were tested ( $\alpha=1, 2$  and  $5$ ). For the  
83 IDW interpolations the implementation in GSTAT was used (Pebesma and Wesseling,  
84 1998).

85 Kriging is a geostatistical interpolation method in which the weights for each  
86 averaged neighbouring data point are defined to minimise the estimation variance  
87 (Matheron, 1963; Journel and Huijbregts, 1978; Cressie, 1990). The minimisation of  
88 this variance enables a spatial covariance criterion to be introduced, which results in  
89 weights for each data point that not only depend on the distance and direction to the grid  
90 cell being estimated (as in IDW), but also on the characteristics of the interpolated  
91 property (described by the variogram,  $V(h)$ , Figure 2) and the relative positions of the

92 averaged hard data (redundancy factor). For the Kriging interpolations the  
93 implementation in GSLIB was used (Deutsch and Journel, 1998).

94 As usual, CV was carried out by temporarily removing an entire well from the  
95 dataset (Deutsch, 2002), but using the model parameters derived from the exhaustive  
96 dataset to execute interpolations. CV error was taken as the average of the absolute  
97 differences between each predicted interpolation estimate and its corresponding real  
98 value. Standard deviation of the CV estimations was used to measure interpolation  
99 smoothing; their relationship is inverse (the higher the standard deviation, the lower the  
100 smoothing). Reference behaviours for the CV comparisons were defined by nearest  
101 neighbour interpolation, and random-based interpolation (i.e. assigning random values  
102 from the input distribution (Figure 1C) considering different degrees of smoothing and  
103 without considering the neighbouring data points preferentially).

### 104 **3. ILLUSTRATION**

#### 105 **3.1. Dataset, interpolation grid and interpolation parameters**

106 The dataset used for illustration derives from the As Pontes Basin (NW Spain), a  
107 small mined non-marine basin (12 km<sup>2</sup>) resulting from the activity of an Oligocene-  
108 Early Miocene strike-slip fault system (Bacelar et al., 1988; Santanach et al., 2005;  
109 Figure 1A). The sedimentary basin fill consists of a 350-400 m thick succession of  
110 siliciclastic facies assemblages alternating and interfingering with coal deposits  
111 (Cabrera et al., 1995, 1996; Falivene et al., 2007a, 2007b), and was extensively drilled  
112 owing to coal mining interest. Lithofacies of the continuously cored exploration wells  
113 were correlated, taking into account the settling and spreading of the major coal seams,  
114 which are bounded by isochronous or near-isochronous surfaces. Several composite  
115 sequences and intervals were identified (Ferrús, 1998; Sáez and Cabrera, 2002; Sáez et

116 [al., 2003](#)). Dry-base calorific values sampled on coal beds in 174 wells drilled through a  
117 30 m-thick, on average, coal-dominated interval (named 6AW, [Falivene et al., 2007a](#))  
118 were used as the input data for the example in this study ([Figure 1B and 1C](#)). These  
119 wells were drilled along a roughly square grid at a spacing of about 105 m. Original  
120 data consisted of more than 2700 calorific value analyses spread over 4000 m of  
121 recovered core. Calorific value distribution in these coals, which form laterally  
122 continuous beds of up to several hundreds of meters, is mainly influenced by the  
123 amount of detritic material, and shows gradual lateral variations ([Figure 1D and 1E](#)).

124 To restore the post-depositional structural deformation ([Santanach et al., 2005](#))  
125 and allow an easier visualization of calorific value distribution, interpolations were  
126 carried out with shifted vertical coordinates transforming the top of the 6AW zone to a  
127 horizontal datum. A grid layering combining proportional and parallel-to-the-top  
128 layering schemes was designed to mimic paleodepositional surfaces, along which  
129 calorific values and facies display the largest continuity ([Figure 1D](#)). Horizontal grid  
130 spacing was set to 20 m. Vertical cell thickness was approximately 0.15 m, in line with  
131 the resolution of core descriptions. Calorific values measured in the cores were upscaled  
132 to the size of grid cells by arithmetic averaging ([Figure 1C](#)), which averaged variability  
133 at smaller scales than the cell size. Upscaled calorific values measured in the coal beds  
134 were then transformed to normal distribution using a normal-scores transformation  
135 ([Deutsch and Journel, 1998](#)). The transformed data were the input for further analyses.

136 Parameters required for interpolation algorithms (i.e. variogram parameters for  
137 Ordinary Kriging and vertical-to-horizontal anisotropy ratios for IDW) were adjusted  
138 from the complete dataset ([Figure 2](#)). Anisotropy ratio ([Jones et al., 1986](#); [Falivene et](#)  
139 [al., 2007a](#)) for IDW was approximated by the vertical-to-horizontal variogram range

140 ratio. This factor is used to multiply the vertical coordinates prior to the interpolation in  
141 order to deal with geometric anisotropy (Kupfersberger and Deutsch, 1999). This  
142 enables assigning different weights to hard data points located at the same real distance  
143 from the point being estimated, but with different stratigraphic position, and allows  
144 reproducing flattened geometries, which are typical of sedimentary deposits.

145 **TENTATIVE POSITION FOR FIGURE 2**

### 146 **3.2. Results**

147 Results were computed directly both for the normal property and after undoing  
148 the normal scores transformation to the original data scale. As both results are  
149 qualitatively similar, for simplicity and geological relevance only the back-transformed  
150 results are shown (Figure 3, 4 and 5). Results in Figure 3 can be summarized as:

151 1) CV error is not independent of smoothing; for random-based interpolation, as  
152 smoothing increases, CV error decreases (Figure 3). Nearest neighbour interpolation  
153 yields the largest CV error and the lowest smoothing with respect to Kriging and IDW  
154 (Figure 3).

155 2) Compared to the results of random-based interpolation, by using average-  
156 based interpolation methods, the CV error and smoothing are always smaller (Figure 3).

157 3) When a small number of neighbouring data points are considered (Figure 4A  
158 and B), the largest CV errors are obtained (Figure 3). If the number of neighbouring  
159 data points increases (Figure 4C and D), then CV error decreases (Figure 3). In IDW,  
160 for very large numbers of neighbouring points, CV error increases slightly.

161 4) Smoothing always increases as the number of neighbours increases (Herzfeld  
162 et al., 1993, Figure 3).

163 5) For IDW, on increasing the power factor, smoothing decreases, whereas CV  
164 error tends to increase (Figure 3B and C). Increasing the power factor increases the  
165 importance of the nearest samples, thus effectively reducing the number of influential  
166 samples in the neighbourhood.

167 6) Depending on the degree of interpolation smoothing (i.e. on the number of  
168 neighbours considered for interpolation), completely different algorithm rankings can be  
169 obtained if only CV error is taken into account (Figure 3B and C).

170 TENTATIVE POSITION FOR FIGURE 3

171 TENTATIVE POSITION FOR FIGURE 4

## 172 4. DISCUSSION AND CONCLUSIONS

173 An optimal interpolation algorithm should provide minimum cross-validation  
174 (CV) error, as is common practice in the literature (Table 1). CV errors in the example  
175 presented here range between 10 to 15% of the mean measured calorific value (Figure  
176 3). These variations are large enough to rank the different algorithms, and can be  
177 significant when predictions are made over large coal volumes. In addition, an optimal  
178 interpolation algorithm should also obtain results with relatively low interpolation  
179 smoothing (Isaaks and Srivastava, 1989; Olea and Pawlowsky, 1996; Journel et al.,  
180 2000), which seeks to preserve as much as possible the gradual lateral variation of  
181 calorific values shown in the mine (Figure 1D, compare Figure 4A to 4C, and 4B to 4D,  
182 Figure 5).

183 TENTATIVE POSITION FOR FIGURE 5



184 Variations in interpolation algorithm rankings, taking only measurements of CV  
185 error (Table 1) have been traditionally justified by the fact that the studied variables are  
186 characterized by different histogram distributions, spatial continuity or sampling  
187 patterns (Brummert et al., 1991; Zimmerman et al., 1999; Lu and Wong, 2008). For  
188 example, a general consensus exists that, in irregularly spaced data, Kriging should  
189 provide more accurate and robust results than IDW, because Kriging takes into account  
190 the relative positions of sampling points, and not only their distance from the  
191 interpolated point (Kane et al., 1982; Lebel et al., 1987; Weber and Englund, 1994;  
192 Borga and Vizzacaro, 1997; Goovaerts, 2000; Falivene et al., 2007a).

193 The results shown herein demonstrate that, if only CV error is considered,  
194 different algorithm rankings can be obtained by changing the number of neighbours  
195 averaged (Figures 3B and 3C). Thus, differences in algorithm rankings cannot be fully  
196 explained by intrinsic differences related to the variable studied and the sampling  
197 patterns, as suggested before. Indeed, interpolation smoothing partially controls the  
198 results of CV error (Figure 3). Interpolation smoothing is primarily controlled by the  
199 number of neighbours averaged, but also by the algorithm itself and other algorithm  
200 parameters (e.g. the semivariogram in kriging and the anisotropy ratio and the power  
201 factor in inverse distance weighting).

202 As a consequence, using only CV error as ranking criteria provides ambiguous  
203 results, because smoothing (relating to each particular algorithm and algorithm  
204 parameters) heavily influences the CV rankings and the appearance and continuity of  
205 the interpolation results (Figure 4 and 5). The interpolation results obtained with the  
206 largest number of neighbours are the ones that yield the lowest CV error, but Figure 4  
207 and 5 shows that the predictions between data points in these cases tend to be too

208 smooth, because of the increasing influence from too much data further away.  
209 Therefore, minimum CV error cannot be the unique criterion of interpolation optimality,  
210 as have been used in previous studies (Table 1). Even for the same interpolation  
211 method, the optimum number of neighbours averaged is not the one that yields  
212 minimum CV errors because the smoothing introduced in the interpolation must also be  
213 taken into account.

214 Multiple-criterion rankings, for instance coupling CV error and smoothing,  
215 needs to be used to search for optimum interpolation strategies. This multi-criterion  
216 would discard too smooth calorific value distributions (i.e. disconnecting large and  
217 small calorific values identified in adjacent wells), such as those in Figure 4D, even  
218 though they may yield the lowest CV error (Figure 3C). And it would favour gradual  
219 and laterally continuous, with moderate CV error and smoothing, such as those in  
220 Figure 4A or 4B (Figure 5). Therefore, in more general terms applicable to other  
221 geological situations or case studies, the analyst should search for a trade-off between  
222 geological continuity (low smoothing) and statistical optimality (low average CV error),  
223 in order to look for best interpolation practices.

## 224 5. ACKNOWLEDGEMENTS

225 Financial support from the Generalitat de Catalunya (Grup de Recerca de  
226 Geodinàmica i Anàlisi de Conques, 2005SGR-000397) and from the MCyT is  
227 acknowledged (Projects CGL2007-66431-C02-01/BTE (MARES 3D/4D) and  
228 CGL2007-66431-C02-02/BTE (REMOSS 3D/4D)). ENDESA MINA PUENTES is  
229 thanked for providing the dataset. Roxar is thanked for providing the IRAP RMS  
230 reservoir modelling software. RT acknowledges funding through the research projects  
231 BPM2003-05640 (MESS) and MTM2006-03040 (MEASURE) of the MEC for the  
232 research group on statistics and data analysis (University of Girona).

## 233 6. REFERENCES

234 Ahlberg, J.H., Nilson, E.W., Walsh, J.L., 1967. The theory of splines and its  
235 applications. Academic Press, New York, 280 pp.

- 236 Bacelar, J., Alonso, M., Kaiser, C., Sanchez, M., Cabrera, L., Sáez, A., Santanach, P.,  
237 1988. La Cuenca Terciaria de As Pontes (Galicia): su desarrollo asociado a  
238 inflexiones contractivas de una falla direccional. II Congreso Geológico de  
239 España, Granada, Sociedad Geologica de España 113-121.
- 240 Bater, C.W., Coops, N.C., 2009. Evaluating error associated with lidar-derived DEM  
241 interpolation. *Computers and Geosciences* 35, 289-300
- 242 Borga, M., Vizzaccaro, A., 1997. On the interpolation of hydrologic variables: formal  
243 equivalence of multiquadratic surface fitting and kriging. *Journal of Hydrology*  
244 195, 160-171.
- 245 Brummert, A.C., Pool, S.E., Portman, M.E., Hancock, J.S., Ammer, J.R., 1991.  
246 Determining optimum estimation methods for interpolation and extrapolation of  
247 reservoir properties: a case study, in Lake, L.W., Carroll, H.B., Wesson, eds.,  
248 *Reservoir Characterization*, pp. 445-485.
- 249 Cabrera, L., Ferrús, B., Sáez, A., Santanach, P., Bacelar, J., 1996. Onshore Cenozoic  
250 strike-slip basins in NW Spain, in Friend, P.F., Dabrio, C.J., eds., *Tertiary*  
251 *Basins of Spain, the Stratigraphic Record of Crustal Kinematics*, pp. 247-254.
- 252 Cabrera, L., Hagemann, H.W., Pickel, W., and Sáez, A., 1995. The coal-bearing,  
253 Cenozoic As Pontes Basin (northwestern Spain): geological influence on coal  
254 characteristics. *International Journal of Coal Geology* 27, 201-226.
- 255 Cressie, N., 1990. The origins of kriging. *Mathematical Geology* 22, 239-252.
- 256 Davis, B.M., 1987. Uses and abuses of cross-validation in geostatistics. *Mathematical*  
257 *Geology* 19, 241-248.
- 258 Davis, J.C., 2002. *Statistics and Data Analysis in Geology*. John Willey & Sons, 638 pp.
- 259 Deutsch, C.V., 2002. *Geostatistical Reservoir Modeling*. Oxford, New York, 376 pp.
- 260 Deutsch, C.V., and Journel, A.G., 1998. *GSLIB: Geostatistical Software Library and*  
261 *User's Guide*, 2nd edition. Oxford University Press, New York, 350 pp.
- 262 Dirks, K.N., Hay, J.E., Stow, C.D., Harris, D., 1998. High-resolution studies of rainfall  
263 on Norfolk Island Part II: interpolation of rainfall data. *Journal of Hydrology*  
264 208, 187-193.
- 265 Dubrule, O., 1984. Comparing Splines and Kriging. *Computers and Geosciences* 10,  
266 327-338.
- 267 Falivene, O., Cabrera, L., Sáez, A., 2007a. Optimum and robust 3D facies interpolation  
268 strategies in a heterogeneous coal zone (Tertiary As Pontes basin, NW Spain).  
269 *International Journal of Coal Geology* 71, 185-208.
- 270 Falivene, O., Cabrera, L., Muñoz, J.A., P., A., Fernández, O., and Sáez, A., 2007b.  
271 Statistical grid-based facies reconstruction and modelling for sedimentary  
272 bodies. Alluvial-palustrine and turbiditic examples. *Geologica Acta* 5, 199-230

- 273 Ferrús, B., 1998. Análisis de cuenca y relaciones tectónica-sedimentación en la cuenca  
274 de As Pontes (Galicia). Unpublished PhD Thesis, Barcelona, University of  
275 Barcelona (Spain), 351 pp.
- 276 Gallichand, J., Marcotte, D., 1993. Mapping clay content for subsurface drainage in the  
277 Nile Delta. *Geoderma* 58, 165-179. Goovaerts, P., 2000. Geostatistical  
278 approaches for incorporating elevation into the spatial interpolation of rainfall.  
279 *Journal of Hydrology* 228, 113-129.
- 280 Herzfeld, U.C., Eriksson, M.G., Holmund, P., 1993. On the Influence of Kriging  
281 Parameters on the Cartographic Output - A Study in Mapping Subglacial  
282 Topography. *Mathematical Geology* 25, 881-900.
- 283 Hutchinson, M.F., Gessler, P.E., 1994. Splines – more than just a smooth interpolator.  
284 *Geoderma* 62, 45-67.
- 285 Isaaks, E.J., Srivastava, R.M., 1989. An introduction to Applied Geostatistics. Oxford  
286 University Press, 561 pp.
- 287 Jones, T.J., Hamilton, D.E., Johnson, C.R., 1986. Contouring geologic surfaces with the  
288 computer. Van Nostrand Reinhold, New York, 314 pp.
- 289 Journel, A., Kyriakidis, P.C., Mao, S., 2000. Correcting the Smoothing Effect of  
290 Estimators: A Spectral Postprocessor. *Mathematical Geology* 32, 787-813.
- 291 Journel, A.G., Huijbregts, C.J., 1978. Mining geostatistics: Academic Press, 600 pp.
- 292 Journel, A.G., Rossi, M., 1989. When do we need a trend in kriging?. *Mathematical*  
293 *Geology* 21, 715-739.
- 294 Kane, V.E., Begovich, C.L., Butz, T.R., Myers, D.E., 1982. Interpretation of regional  
295 geochemistry using optimal interpolation parameters. *Computers and*  
296 *Geosciences* 8, 117-135.
- 297 Kupfersberger, H., Deutsch, C.V., 1999. Methodology for Integrating Analog Geologic  
298 Data in 3-D Variogram Modeling. *American Association of Petroleum*  
299 *Geologists Bulletin* 83, 1262-1278.
- 300 Lebel, T., Bastin, G., Obled, C., Creutin, J.D., 1987. On the accuracy of rainfall  
301 estimation: a case study. *Water Resources Research* 23, 2123-2134.
- 302 Lu, G.Y., Wong, D.W., 2008. An adaptive inverse-distance weighting spatial  
303 interpolation technique. *Computers and Geosciences* 34, 1044-1055.
- 304 Matheron, G., 1963. Principles of geostatistics. *Economic Geology* 58, 1246-1266.
- 305 Mitsova, H., Mitsova, L., 1993. Interpolation by regularized spline with tension: I.  
306 Theory and implementation. *Mathematical Geology* 25, 641-655.
- 307 Morrison, J.L., (1974). Observed statistical trends in various interpolation algorithms  
308 useful for first stage interpolation. *The Canadian Cartographer* 11, 142-159.

- 309 Moyeed, R.A., Papritz, A., 2002. An Empirical Comparison of Kriging Methods for  
310 Nonlinear Spatial Point Prediction. *Mathematical Geology* 34, 365-386.
- 311 Okubo, C.H., Schultz, R.A., Stefanelli, G.S., 2004. Gridding Mars Orbiter Laser  
312 Altimeter data with GMT: effects of pixel size and interpolation methods on  
313 DEM integrity. *Computers and Geosciences* 30, 59-72.
- 314 Olea, R., Pawlowsky, V., 1996. Compensating for estimation smoothing in kriging.  
315 *Mathematical Geology* 28, 407-417.
- 316 Pebesma, E.J., Wesseling, C.G., 1998. GSTAT: A program for geostatistical modelling,  
317 prediction and simulation. *Computers and Geosciences* 24, 17-31.
- 318 Sáez, A., Cabrera, L., 2002. Sedimentological and paleohydrological responses to  
319 tectonics and climate in a small, closed, lacustrine system: Oligocene As Pontes  
320 Basin (Spain). *Sedimentology* 49, 1073-1094.
- 321 Sáez, A., Inglès, M., Cabrera, L., de las Heras, A., 2003. Tectonic-palaeoenvironmental  
322 forcing of clay-mineral assemblages in nonmarine settings: the Oligocene-  
323 Miocene As Pontes Basin (Spain). *Sedimentary Geology* 159, 305-324.
- 324 Santanach, P., Ferrús, B., Cabrera, L., Sáez, A., 2005. Origin of a restraining bend in an  
325 evolving strike-slip system: The Cenozoic As Pontes basin (NW Spain).  
326 *Geologica Acta* 3, 225-239.
- 327 Teegavarapu, R.S.V., Chandramouli, V., 2005. Improved weighting methods,  
328 deterministic and stochastic data-driven models for estimation of missing  
329 precipitation records. *Journal of Hydrology* 312, 191-206.
- 330 Weber, D.D., Englund, E.J., 1992. Evaluation and comparison of spatial interpolators.  
331 *Mathematical Geology* 24, 381-391.
- 332 Weber, D.D., Englund, E.J., 1994. Evaluation and comparison of spatial interpolators II.  
333 *Mathematical Geology* 26, 589-603.
- 334 Zimmerman, D., Pavlik, C., Ruggles, A., Armstrong, P., 1999. An experimental  
335 comparison of ordinary and universal kriging and inverse distance weighting.  
336 *Mathematical Geology* 31, 375-390.

337 **FIGURE AND TABLE CAPTIONS**

338 **Table 1.** Summary of the results from published interpolation algorithm comparisons by  
339 means of the cross-validation (CV) check.

340 **Figure 1.** Geological setting and dataset characteristics. **(A)** Present basin boundary and  
341 areal extent of the studied 6AW interval. Coordinates are in kilometres; see location of  
342 the basin in the upper right inset. **(B)** Well distribution in the 6AW interval. The  
343 location of the reference section in [Frames D and E](#) and in [Fig. 4](#) is shown. **(C)** Relative  
344 frequency of calorific values; plotted information corresponds to the core data upscaled  
345 to the size of grid cells. **(D)** Reference section showing upscaled calorific values in the  
346 intersected wells; calorific values in lacustrine and alluvial mudstone are null.  
347 Approximate paleodepositional surfaces are shown. **(E)** Facies distribution in the coal  
348 zone obtained by using indicator Kriging with an areal trend applied to categorical  
349 variables (for details, see [Falivene et al., 2007a](#)). Vertical exaggeration of [Frames D and](#)  
350 [E](#) is 10x.

351 **Figure 2.** Variograms for the transformed calorific values. Black dots, crosses and  
352 dashed curves correspond to the experimental variograms derived from upscaled well  
353 data. Grey continuous curves to the theoretical model fitted ( $H_r$  and  $V_r$  stand for  
354 horizontal and vertical ranges, respectively):  $V(h) = 0.82 \cdot \text{Exp}(H_r = 450\text{m}, V_r = 2.8\text{ m})$   
355  $+ 0.18 \cdot \text{Exp}(H_r = 60\text{m}, V_r = 100\text{m})$ .

356 **Figure 3.** Interpolation smoothing (measured by the standard deviation of cross  
357 validation (CV) estimates) against mean absolute CV error for all the interpolation  
358 strategies compared. The greater the standard deviation, the lower the smoothing;  
359 standard deviation in the original dataset was 650. **(A)** Results for several numbers of  
360 averaged neighbours (2, 4, 12, 24, 48, 96, 192 and 288). Note also the results of the  
361 nearest neighbour and random-based interpolations (i.e. assigning random values from  
362 the input distribution (with different smoothing degrees), and without considering the  
363 neighbouring points. **(B)** Detail with the results for 12 averaged neighbours. **(C)** Detail  
364 with the results for 192 averaged neighbours. Note the correspondences with frames in  
365 [Figure 4](#).

366 **Figure 4. (A, B, C, D)** Reference section and map showing calorific value distributions  
367 in coal facies obtained by different interpolation strategies. Calorific value in alluvial  
368 and lacustrine mudstone facies shown in [Figure 1E](#) is null. **(E)** Location of the section,  
369 the map and the input data. Note that the horizontal scale of the map and the section are  
370 not the same. If the number of averaged neighbours increases, the spatial continuity of  
371 the resultant calorific value distribution in coal facies is obscured, as the result of larger  
372 interpolation smoothing. Vertical exaggeration 10x.

373 **Figure 5.** Calorific values for those cells in the intersection of the map and the section  
374 shown section in [Figure 4](#), obtained by different interpolation strategies. Note that too  
375 smooth interpolation methods such as Kriging or IDW with 192 averaged neighbours  
376 provide interpolations that in some cases deviate largely from the closest surrounding  
377 data due to the effect of data located further away, although they yield lower CV errors  
378 than algorithms considering a smaller number of averaged neighbours.

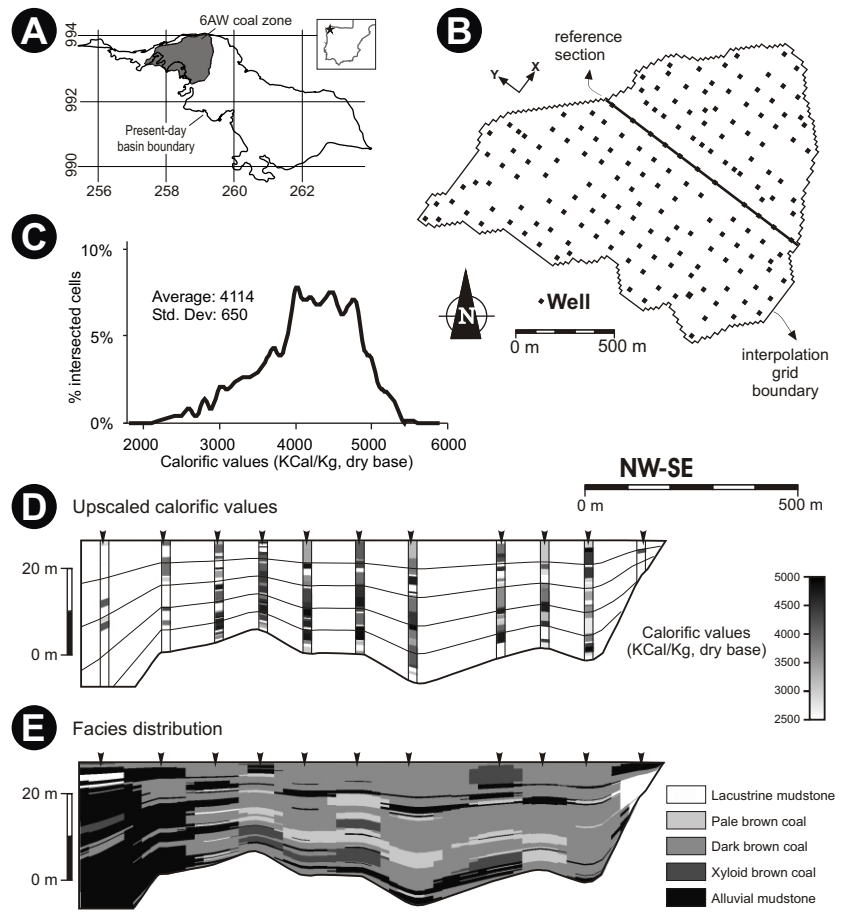
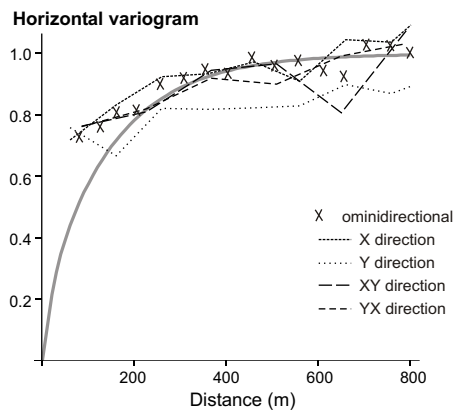
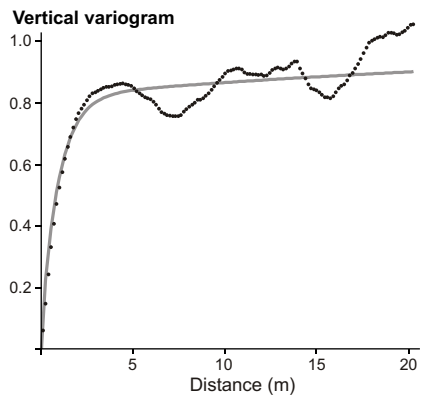


Figure 1.



**Figure 2.**



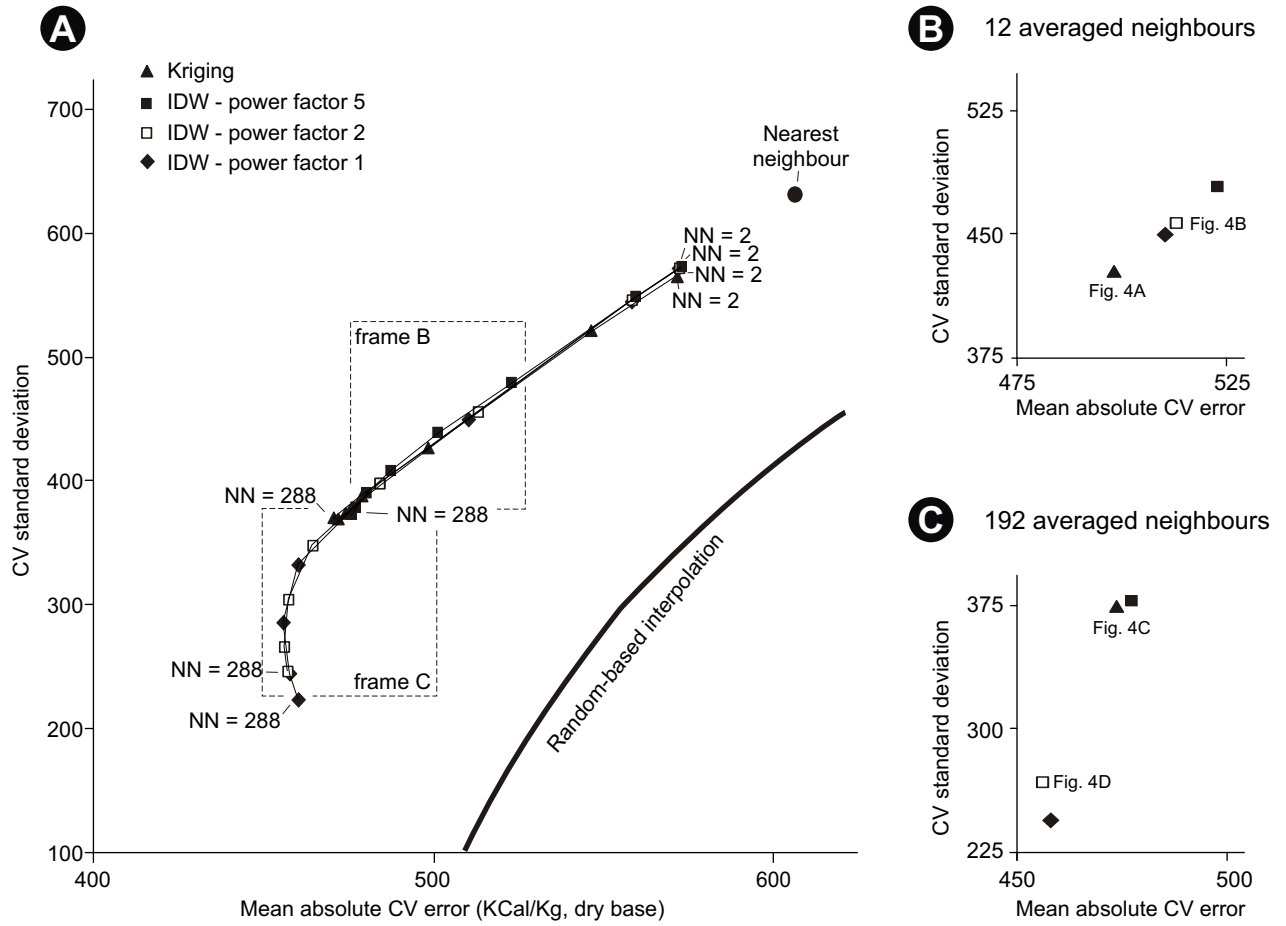


Figure 3.

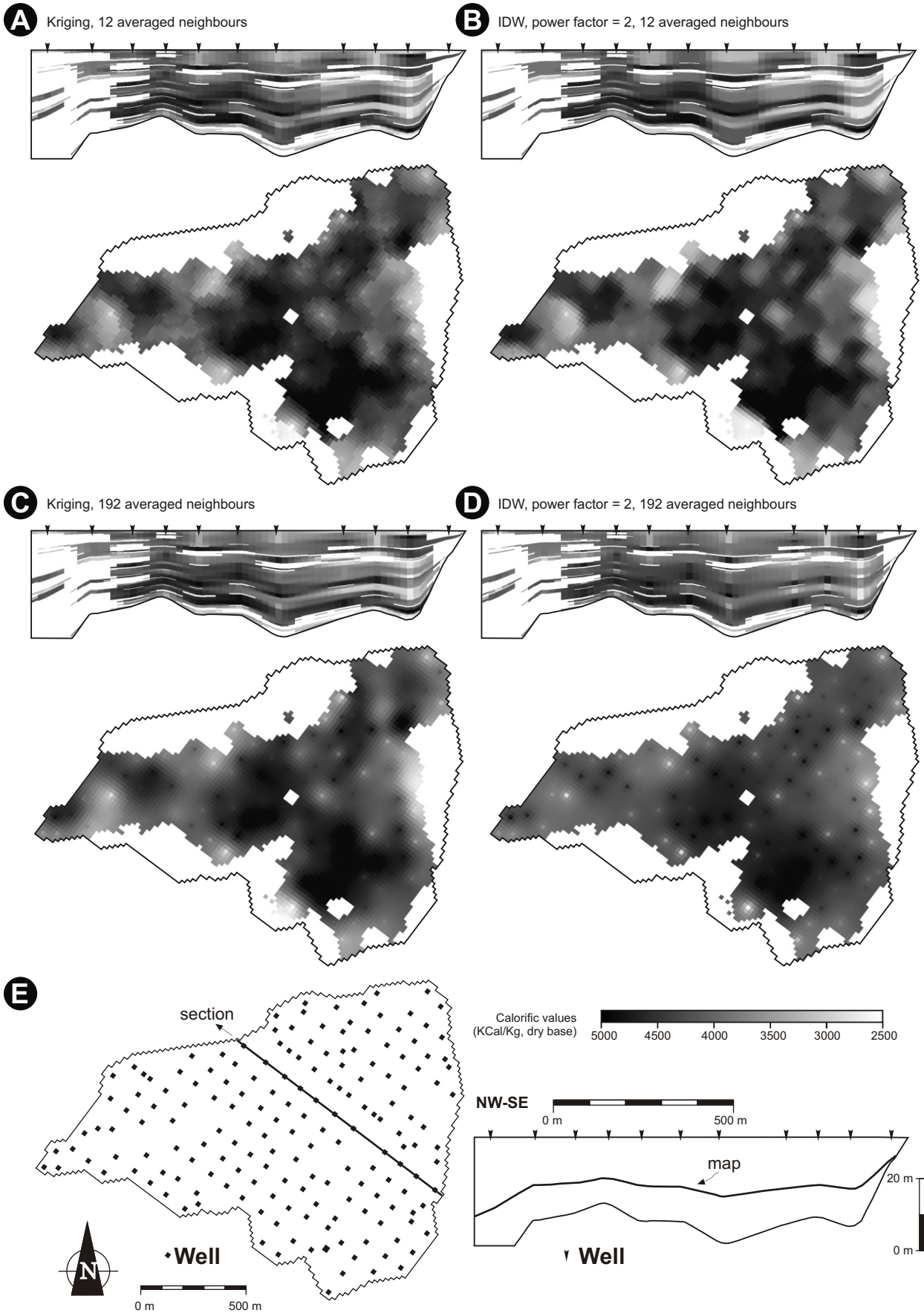


Figure 4.

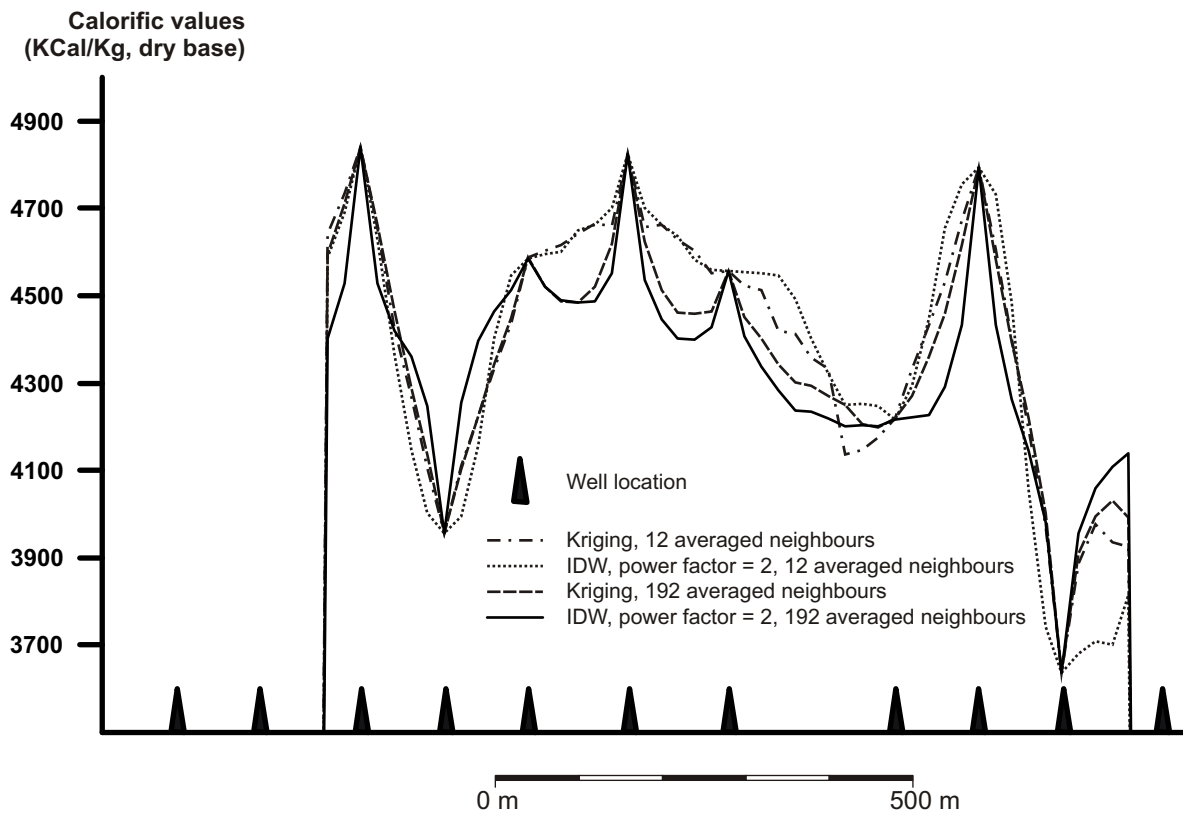


Figure 5.

**Supplementary Material Captions**

[Click here to download e-component: Supplementary Material Captions.doc](#)

**Supplementary Material**

[Click here to download e-component: CP\\_IDW\\_012.wri](#)

**Supplementary Material**

[Click here to download e-component: CP\\_IDW\\_192.wri](#)

**Supplementary Material**

[Click here to download e-component: CP\\_Kriging\\_012.wrl](#)

**Supplementary Material**

[Click here to download e-component: CP\\_Kriging\\_192.wrl](#)